

# Active flow control of laminar separation bubbles on a rectangular wing using micro synthetic jets

Wei Zuo, Yunsong Gu\*

Nanjing University of Aeronautics and Astronautics, College of Aerospace Engineering, Nanjing, China

\*yunsonggu@nuaa.edu.cn

## Abstract

Active control of flow over a NACA633-421 rectangular wing model at  $Re=1.2E5$ , based on the free-stream velocity  $U_\infty$  and airfoil chord length  $c$ , is carried out for laminar separation bubble (LSB) suppression using a micro time-periodic synthetic jet from slits on the wing surface. The experiments are conducted in a low-noise and low turbulence level wind tunnel available at Nanjing University of Aeronautics and Astronautics. The forcing frequency  $f$  and velocity amplitude  $v_{amp}$  of the micro synthetic jet (Micro-SJ) are changed in the experiments and control effects are contrasted under three different working conditions of Micro-SJ: ConA:  $fc/U_\infty=10.5$ ,  $v_{amp}/U_\infty=0.0045$ ; ConB:  $fc/U_\infty=10.5$ ,  $v_{amp}/U_\infty=0.2$ ; ConC:  $fc/U_\infty=28.1$ ,  $v_{amp}/U_\infty=0.2$ . With the forcing, LSB on the wing disappears significantly for the forcing frequency approximately equal to a critical frequency (about  $10U_\infty/c$ ). The critical forcing frequency is found to be closely associated with the onset of the separated shear layer instability. It is shown from the surface-pressure measurement, off surface visualization with particle image velocimetry (PIV) and near-wall streamwise velocity measurement with hotwire that the disturbances from Micro-SJ of specific frequency grow inside the boundary layer, and they grow further along the separated shear layer and high momentum in the free stream is entrained toward the wing surface, resulting in the reattachment point moving forward. Time-averaged PIV velocity map demonstrates that the length of LSB is shortened from  $20\%c$  to  $13\%c$  with Micro-SJ control under ConC while the LSB almost disappears under the other two flow control conditions of ConA and ConB. Phase-locked PIV results and power spectra analysis of hotwire signals reveal the differences of flow field structure with and without Micro-SJ control, along with perturbation growth process clearly.

## 1 Introduction

According to requirements of intelligence and reconnaissance missions, the development of high altitude long endurance unmanned aerial vehicles (HAHE UAV) has drawn more and more researchers' attention, Qiu, Yuxin (2004). HAHE UAV typically cruises at 0.5-0.8 Mach, corresponding to relatively low Reynolds numbers between  $10^4$  and  $10^5$ . Besides, the flow on the surface of MAV, wind turbine and compressor is usually in this low Reynolds number range. At low Reynolds numbers, when a laminar boundary layer cannot overcome the viscous effects and adverse pressure gradients, it separates from the wall and transition as a result of Kelvin-Helmholtz instabilities may occur in the separated shear layer and may reattach to the surface forming a laminar separation bubble (LSB), Horton (1968), Gaster (1969) and Mueller et al (1982). From the pioneering work, we know that the laminar-to-turbulent transition process in the separated shear layer is a key feature of airfoil boundary-layer development at low Reynolds numbers. Flow transition in the separated shear layer on the upper surface of a NACA 0025 airfoil at low Reynolds numbers investigated by Yarusevych (2008) (2009) declares that transition occurs due to the amplification of natural disturbances within a band of frequencies centered at some fundamental frequency. The growing disturbances also cause shear-layer rolling up and the formation of roll-up

vortices at the last stage of transition, which results in rapid flow breakdown to turbulence. The process of roll-up vortices emerging, merging and breakdown also have been analyzed through time-resolved particle-image velocimetry (TR-PIV), stereo-scanning particle-image velocimetry (SPIV) flow visualization, e.g., in Burgmann (2006) (2008). Numerical simulation result of the E387 airfoil near the trailing-edge at low Reynolds number from BAI Peng (2006) also verifies the great importance of the periodical vortex shedding and incorporation proceed to the laminar separation bubble structure<sup>[9]</sup>.

It is known from the literature that the appearance of a separation bubble significantly decreases the airfoil performance sharply, Fitzgerald and Mueller (1990), Mohamed G (2001) e.g., a reduction of lift, an increase of drag, buffeting, or even stall occurring. In addition, the non-linear effects of the aerodynamic coefficients at the small angle of attack and the non-linear static hysteresis at the middle and large angle of attack due to the appearance of LSB also have drawn researchers' attention and are investigated through experiments and numerical calculations, Mueller (1985), Hu Hui (2007) and Bai Peng (2015). Then how to improve the aerodynamic characteristics of airfoils at low Reynolds numbers becomes increasingly important. Active flow control (AFC) comes into researchers' view as it can manipulate many different complex flows in which case passive flow control (PFC) usually could do nothing, at a fraction of the cost. Synthetic jet (SJ), as a popular AFC method, has been studied and applied into flow over a wing at high angles of attack and S-shaped inlet producing a separation suppression. It's worth mentioning that the work by Smith BL & Glezer A(1997) and Amitay, Smith BL & Glezer A(1998) shows that the application of a high-frequency forcing from a synthetic jet to flow over a circular cylinder produces a significant drag reduction at sub-critical Reynolds numbers, and they attributes the mechanism to the 'virtual aero-shaping'. That is, the interaction of synthetic jets with an external cross-flow leads to the formation of a separation bubble and thus apparent modification of the surface shape.

Micro synthetic jet (Micro-SJ), characterized by very small jet momentum, is applied in the present study for LSB control on a rectangular wing at low Reynolds numbers. Micro-SJ provides a time-periodic forcing disturbance from a slit located before the separation line. The main objective of the present study is to investigate how different frequencies forcing changes the shear layer characteristics after separation and how this change eliminates LSB flow structure. Another objective is to see which one is the key control parameter. The effect of Micro-SJ control on the flow field near the rectangular wing is detailedly investigated through PIV flow visualization and hot-wire dynamic signals analysis. Dynamic behavior of separated shear layer with and without control will be a key focus of this investigation.

## 2 Experimental apparatus

Experimental investigations were performed in a low turbulence and low noise recirculating open-type wind tunnel of NAAA. The 1.7-m-long test section of this tunnel has a spanwise extent of 1.5m and a height of 1m and the background turbulence intensity level in the test section is less than 0.1%. The stable free-stream velocity ranges from 0.5m/s to 30 m/s. The NACA63<sub>3</sub>-421 rectangular wing model made of steel tested in the wind tunnel has a chord length of  $c=246$  mm and a spanwise length of  $l=500$ mm. Six SJ actuators equidistantly in spanwise are built in wing model and six jet slit pairs are  $0.3c$  from the leading edge on the upper surface. Every slit has a length of  $l_s=15$ mm and width of  $w=1$ mm (see Figure1). As mentioned before, this experiment consists of two parts, 2-D PIV flow field measurement near upper surface and hot-wire dynamic data acquisition of shear layer. Based on the premier result analysis of pressure distribution on upper surface, the test region of interest is chosen from  $0.5c$  to  $0.9c$  at the  $0.57l$  spanwise section from wing root to cover the whole separation bubble. PIV system produced by TSI includes VLITE200 laser (200mJ/pulse), 14bit CCD camera (1376pixel $\times$ 1024pixel), 610035 synchronizer and INSIGHT 3G software. In this PIV experiment, exposure frequency rate of laser is 10Hz. Instantaneous PIV velocity vectors are obtained by a frame to frame cross-correlation technique involving successive frames of patterns of particle images in an interrogation window  $32\times 32$  pixels.

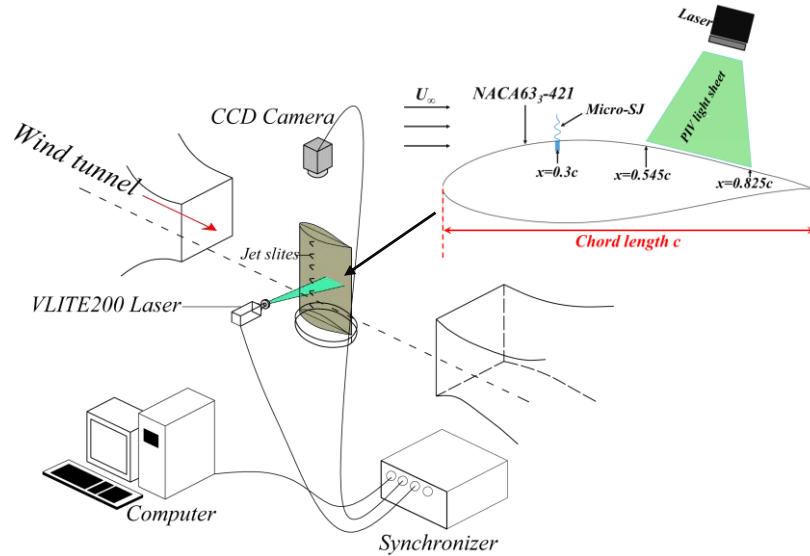


Figure1: Schematic diagram of PIV experimental set-up

Table 1: Experiment parameter

Parameter	Symbol	Value
Airfoil		NACA63 <sub>3</sub> -421
Span length	$l$	500 mm
Chord length	$c$	246 mm
Free-stream velocity	$U_\infty$	7 m/s
Reynolds number	$Re$	1.2E5
Angle of attack	$\alpha$	0 °

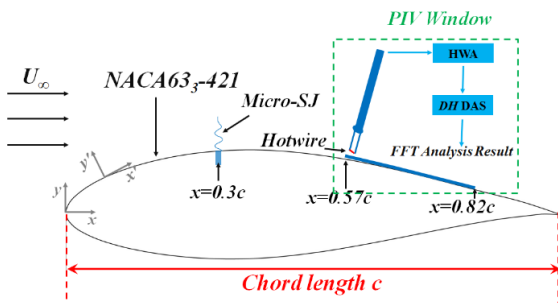


Figure 2: Schematic view of hotwire dynamic test

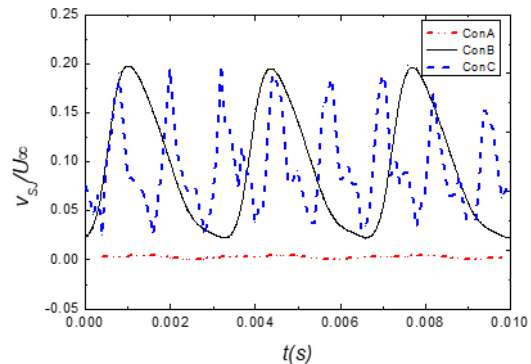


Figure 3: Illustration diagram of three different Micro-SJ control conditions

Figure 2 shows us the whole test process that how to acquire the dynamic flow signals of shear layer. A tiny hot-wire probe is set close to the wing surface carefully, while hot wire anemometer (HWA) in charge of accurately acquiring voltage values from hotwire, the device called DH Data Acquisition Station (DH DAS) responsible for the analysis and output of dynamic voltage signals. Sampling frequency in present experiment is set for 5K Hz constantly, while other experimental parameters stay the same with PIV experiment.

Control effects are contrasted under three different working conditions of Micro-SJ: ConA:  $fc/U_\infty=10.5$ ,  $v_{amp}/U_\infty=0.0045$ ; ConB:  $fc/U_\infty=10.5$ ,  $v_{amp}/U_\infty=0.2$ ; ConC:  $fc/U_\infty=28.1$ ,  $v_{amp}/U_\infty=0.2$ . Figure 3 shows the temporal variations of the Micro-SJ velocity  $v_{SJ}$  measured at jet slits using a single hot-wire

probe. On one hand, the maximum velocity  $v_{amp}$  (or forcing amplitude) at the slit is tuned to be  $0.2U_\infty$  both in ConB and ConC. On the other hand, ConA and ConB have the same frequency  $f=10.5U_\infty/c$  which approaches the critical frequency  $f_0$  of shear layer instability (see Table2).

Table 2: Micro-SJ Control Parameter

Condition	$f$ (Hz)	$f_0$ (Hz)	$fc/U_\infty$	$v_{amp}/U_\infty$
ConA	300	250,350	10.5	0.0045
ConB	300	250,350	10.5	0.2
ConC	800	250,350	28.1	0.2

### 3 Results and discussion

#### 3.1 Flow field visualization

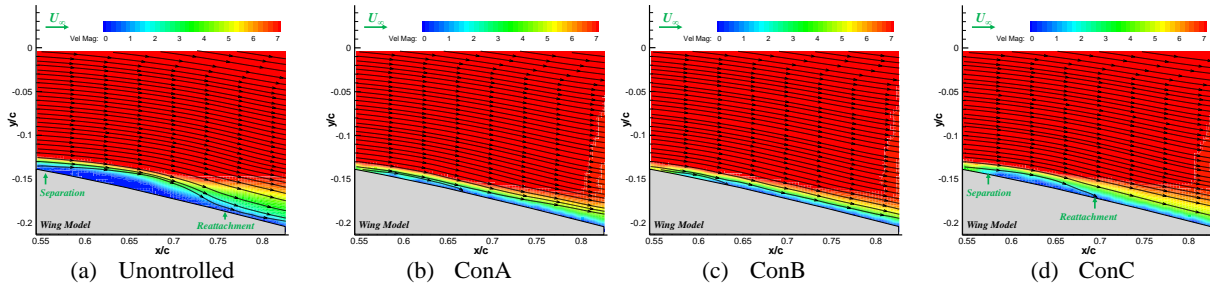


Figure 4: Streamlines and velocity magnitude distribution over up surface flow of a NACA633-421 rectangular wing with and without Micro-SJ control (Time-averaged PIV measurements,  $Re=1.2E5$ ,  $\alpha=0^\circ$ )

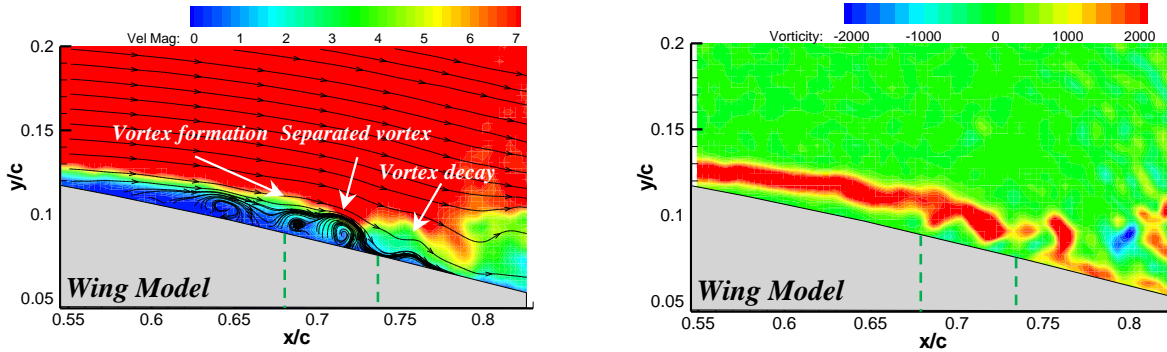


Figure 5: Contours of instantaneous velocity (left) and vorticity (right) over up surface flow of a NACA633-421 rectangular wing

Time-averaged velocity contours obtained from a cinema sequence of 200 frames of instantaneous velocity fields shows us a typical laminar separation bubble flow structure on upper surface of the NACA63<sub>3</sub>-421 rectangular wing at  $Re=1.2E5$  and  $\alpha=0^\circ$ . Flow has separated from surface at  $x=0.55c$ , evolving into separated shear layer subsequently and attaches to the airfoil approximately at  $x=0.74c$  again. A  $20\%c$  long and  $1.5\%c$  high closed bubble-like structure of flow separation is generated. On the right of figure 4, the strong rotational flow zone of large vorticity presents the separated shear layer. It is observed that time-averaged flow in our study behaves in keeping with classical LSB model proposed by Horton(1968).

The instantaneous velocity magnitude distribution over up surface flow of the NACA63<sub>3</sub>-421 rectangular wing is depicted in figure 5, which gives us some details about the laminar-to-turbulent transition process in the separated shear layer. We can see that the separated shear layer is not so stable as time-averaged result actually and it develops downstream along with the presence of roll-up vortices at  $x=0.68c$ . Further downstream, roll-up vortices start shedding and come into a breakdown approximately at

the position of reattachment. During this process, the separated shear layer comes into swaying at  $x=0.68c$  due to K-H instability. Furthermore, shear layer flaps to the surface quasi-periodically to form a time-averaged reattachment. Thus, it can be concluded that the process of transition and reattachment is accompanied by the roll-up and decay of vortex structures, in which case the investigation on the dynamic behavior of separated shear layer becomes very necessary.

As revealed in the time-averaged PIV measurement results given in Figure 4, small disturbances from Micro-SJ control have altered the flow structure on upper surface of NACA 63<sub>3</sub>-421 wing significantly. After flow control, laminar separation is dismissed (in ConA and ConB) or delayed (in ConC) compared with flow field without control at low Reynolds numbers. In ConA and ConB of which control frequency is  $f=10.5U_\infty/c$ , shear layer adjoins the wall instead of flapping violently far away wall which always results in a terrible handling characteristic for air vehicles. In addition, phase-locked flow field PIV visualization also shows us that the shear layer takes a stable and time-periodic fluctuation up and down within a narrow range close to the wing surface. In ConC of which control frequency is  $f=28.1U_\infty/c$ , laminar separation bubble structure still exists while the length of LSB is shortened by  $7\%c$ . Obviously, active flow control by Micro-SJ achieves a remarkable effect in LSB suppression and forces flow to be stable at low Reynolds number. Furthermore, it is also concluded that control frequency plays an important role in control effect by contrasting three different conditions. When forcing frequency is fit for separated shear layer, the perturbation will make a difference in flow field even if it was so tiny (see ConA).

### 3.2 Profile of velocity shape

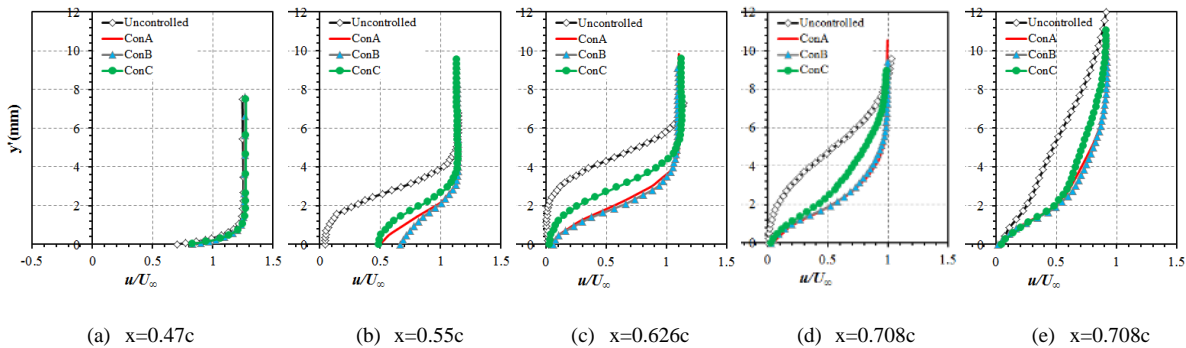


Figure 6: Profile of velocity shape at different streamwise positions with and without Micro-SJ control

Figure 6 shows the profiles of the mean streamwise velocity extracted from PIV measurement along the normal direction from the airfoil surface at  $x=0.47c\sim 0.8c$ . For the case of the basic wing, a thin boundary-layer flow is formed at  $x=0.47c$ , but the flow is detached from the wall at  $x=0.55c$ , showing that separation occurs between  $x=0.47c$  and  $0.55c$ . In the case of high-frequency Micro-SJ control ( $f=28.1U_\infty/c$ ), the near-wall velocity gradient at  $x=0.47c$  is a little larger and the shear-layer thickness after separation (at  $0.626c$  and  $0.708c$ ) is smaller than those in the case of the basic wing, implying that separation is slightly delayed owing to the high-frequency forcing. The separation region is limited very near the wall because the flow has a high momentum outside. Because of flow control, the separated shear layer in the case of high-frequency forcing reattaches to the wall earlier than in the case of the basic wing; the shear layer reattaches at  $x=0.708c$  in the case of high-frequency forcing, as shown in figure 6.

In case of the relative low-frequency control ( $f=10.5U_\infty/c$ ), the flow maintains laminar boundary-layer characteristics up to  $x=0.626c$ , i.e. a thin boundary layer and non-broadband power spectrum (see below). Besides, the separation region disappears near the wall because the shear layer moves downstream nestled against the wall and flow has a high momentum outside. Note that the profiles of velocity shape are almost the same in the case of ConA and ConB, even though the jet velocity amplitude is much higher in the latter case, indicating that the streamwise velocity is nearly insensitive to the forcing amplitude, at least in the range of  $0.005 \leq v_{amp}/U_\infty \leq 0.2$ .

### 3.3 Dynamic performance of LSB

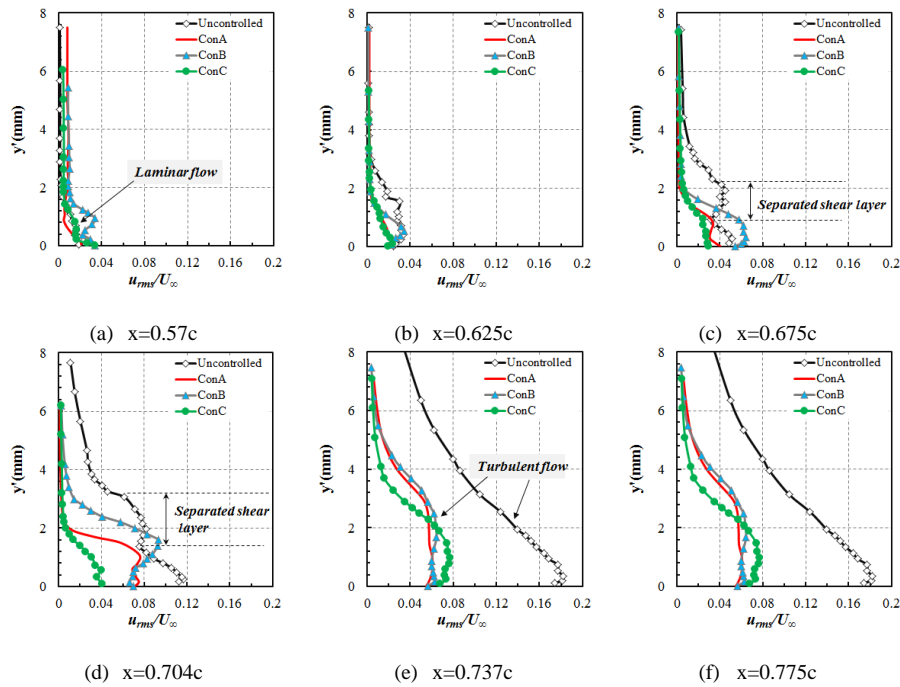


Figure 7: Profile of velocity fluctuation near wall at different chord positions with and without Micro-SJ control

As mentioned above in PIV result discussion, the flow structure of a LSB is actually an averaged consequence of the process of vortex formation, vortex shedding and vortex decay, so it is necessary to explore the dynamic performance of LSB. Figure 7 shows the profiles of the root-mean-square velocity fluctuations ( $u_{rms}$ ) measured with a hot-wire probe along the normal direction from the upper surface at  $x=0.57c\sim 0.78c$ . In the basic case without control, when the shear layer separates from wall at the beginning, it keeps in laminar flow of which velocity fluctuation is very small and  $u_{rms}$  increases slowly along streamwise. At  $x=0.675c$ , when the normal distance from wall  $y' < 0.8\text{mm}$ ,  $u_{rms}$  decreases as  $y'$  increases due to the effect of wall. When  $0.8\text{mm} < y' < 2\text{mm}$ , the high level of velocity fluctuations represents the intense shear of separated flow, corresponding to a separated shear layer of LSB. At  $x=0.704c$ ,  $u_{rms}$  has a sharp augment which indicates the flow transits into turbulence and the width of separated shear layer zone becomes greater owing to the development of roll-up vortices scale. When downstream to  $0.737c$ , the level of  $u_{rms}$  further increases and the shear layer reattaches to the surface in turbulent status. At  $x=0.775c$ , the significant increase of  $u_{rms}$  compared with  $x=0.737c$  can be attributed to the severe flap of shear layer, inducing violent momentum exchanges in the flow field near wall.

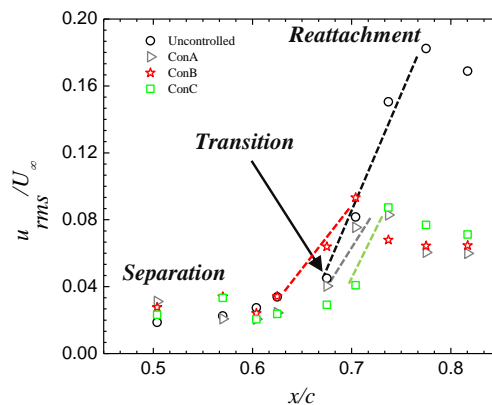


Figure 8: Maximum of velocity fluctuation near wall at different chord positions with and without Micro-SJ control

In case of Micro-SJ control, the high-level velocity fluctuation zone still exists but close to wall, demonstrating none of obvious separation. Due to the reduced swing scope of shear layer after control, the velocity fluctuations have an apparent drop with respect to the case without control from  $x=0.737c$  to  $x=0.817c$  (see Figure 8), showing that shear layer is forced to keep stable relatively in the case of time-periodic forcing from Micro-SJ. Figure 8 shows the maximum of  $u_{rms}$  variation along the streamwise direction, which can help us judge the various stages in the process of the LSB structure formation clearly. In the first stage of  $x < 0.675c$ , the maximum of  $u_{rms}$  keeps in a very low level without apparent increase downstream, indicating laminar separated shear layer. At  $0.675c < x \leq 0.775c$ , the maximum of  $u_{rms}$  increases rapidly on behalf of the second stage of transition into turbulence, and the energy from free stream is taken in under the intense shear stress.  $x > 0.775c$  is the last stage, showing the reattachment of separated shear layer. Obviously, the discussion about LSB structure on the basis of its dynamic behavior is consistent with PIV visualization result.

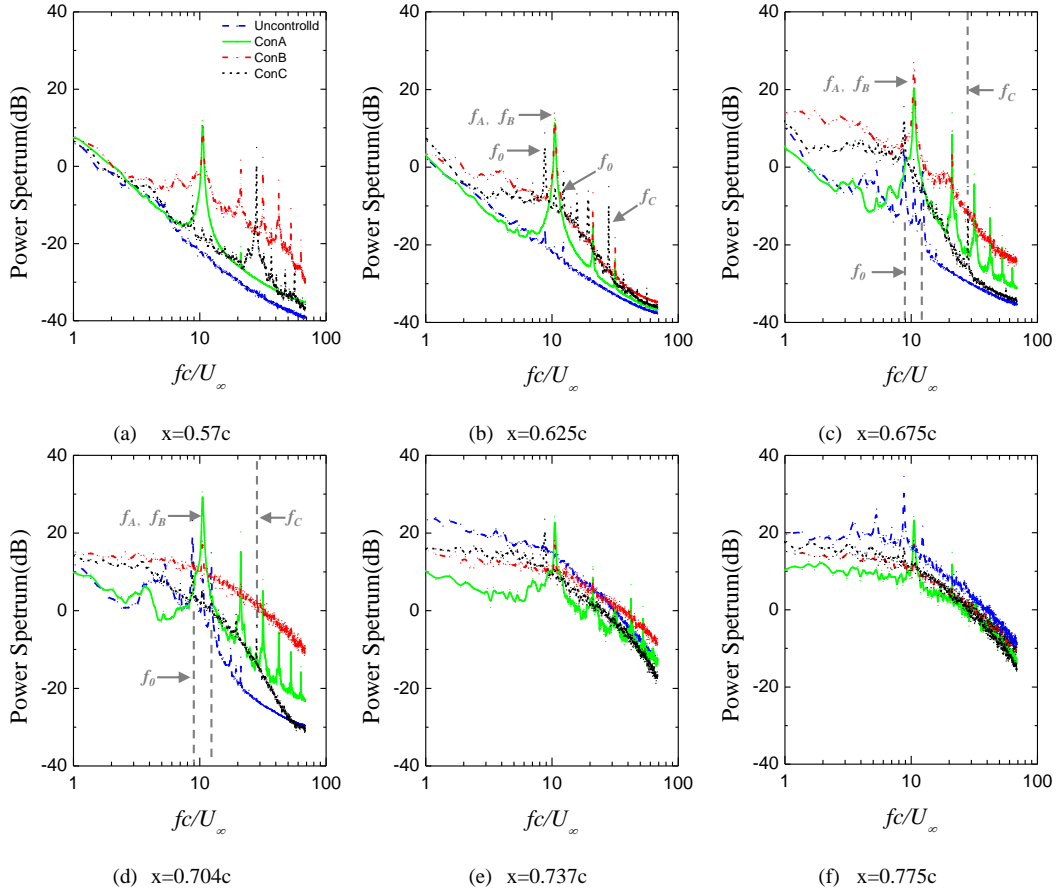


Figure 9 Power spectra of the streamwise velocity at the location of having maximum  $u_{rms}$   
 ConA:  $fc/U_\infty=10.5$ ,  $v_{amp}/U_\infty=0.0045$ ; ConB:  $fc/U_\infty=10.5$ ,  $v_{amp}/U_\infty=0.2$ ; ConC:  $fc/U_\infty=28.1$ ,  $v_{amp}/U_\infty=0.2$

At each position, the streamwise velocity signal at the normal location where  $u_{rms}$  is maximum is Fourier-transformed to obtain its power spectrum. Figure 9 shows the power spectra of velocity fluctuation at  $x=0.57c \sim 0.775c$  for  $Re=1.2E5$  at  $\alpha=0^\circ$  for the case of the basic and Micro-SJ control case. For the basic wing, figure 10 shows the characteristics of laminar and transitional flows and two distinct peaks at  $f_0=8.8U_\infty/c$ ,  $12.3U_\infty/c$  observed for  $x=0.675c$  clearly indicate the roll-up vortices frequency, which is same with the frequency of shear layer instability. In particular, disturbances within a band of frequencies, centered at a fundamental frequency  $f_0$  are amplified in the separated shear layer. The initial growth of the disturbances is followed by the generation and growth of harmonics and a sub-harmonic of the fundamental frequency, which is indicative of nonlinear interactions between the disturbances, Dovgal

AV (1994). This is followed by a rapid laminar-to-turbulent transition, with a ‘classical’ turbulence spectrum observed in the aft portion of the separated flow region.

For the Micro-SJ control of ConA and ConB, the peaks are found at the control frequency and its harmonic frequencies. In ConB, the shear layer flow is more likely to be a laminar-to-turbulent process without separation, and the energy at forcing and its harmonic frequencies increases very rapidly from  $x=0.57c$  and the spectrum becomes broadband between  $x=0.675c$  and  $x=0.704c$ , which indicates that fluctuations rapidly increase at all scales along the shear layer, resulting in the total transition to turbulence of the flow on the wing surface. In ConA, the increasing rate of forcing control signal in shear layer appears slower with respect to ConB and its spectrum totally becomes broadband up to  $x=0.737c$ . For the case of ConC, both the peak at critical frequency  $f_0$  and the peak at forcing frequency  $f_c$  are found in the power spectra, and the transition point is brought forward from  $x=0.675c$  (basic case) to  $x=0.625c$  (ConC), indicating that the high-frequency Micro-SJ forcing promotes the transition of separated shear layer. However, the energy of forcing frequency  $f_c$  decreases downstream in shear layer from  $x=0.57c\sim 0.704c$ .

## 4 Conclusion

In the present study, an active flow control over a rectangular wing was conducted for LSB suppression using micro synthetic jets at a sub-critical Reynolds number of  $Re=1.2E5$ . Both the static performance and dynamic behavior of LSB flow structure with and without control were investigated to explore the effects of Micro-SJ time-periodic forcing to flow field.

By contrasting instantaneous and time-averaged velocity field, it is shown that the shear layer becomes unstable travelling downstream after separation, inducing the formation of roll-up vortices, further leading to the separated shear layer flapping along with vortices shedding and vortices decay at the critical frequencies of  $f_0=8.8U_\infty/c$ ,  $12.3U_\infty/c$ . The sharp flapping to the wall of shear layer results in the flow reattaching to upper surface, with the ending of flow separation, forming a bubble-like flow structure at low Reynolds numbers.

The time-periodic Micro-SJ forcing is proved to be beneficial to the flow field over the rectangular wing, eliminating laminar separation totally (ConA and ConB) or shortening the length of LSB by 7%. Forcing frequency of Micro-SJ seems to play a highly important role in control effects. When control frequency  $f$  approaching to the critical frequency of shear layer instability  $f_0$ , Micro-SJ even if with very small jet velocity amplitude still makes difference in LSB suppression, driving shear layer swaying weakly close to the wall instead of separating.

## Acknowledgements

This work was supported by the National Natural Science Foundation of the Peoples’ Republic of China with Grant No. 11672134.

## References

- Qiu YX, Cheng YH and Xu JC (2004) A brief discussion of high-altitude long-endurance unmanned aerial vehicle aerodynamic research. *Experiment and measurement of fluid mechanics* 18.3: 1-5.
- Horton HP (1968) Laminar separation bubbles in two and three dimensional incompressible flow. Diss.
- Michael G (1969) The structure and behaviour of laminar separation bubbles. HM Stationery Office.
- Mueller TJ and Batil SM (1982) Experimental studies of separation on a two-dimensional airfoil at low Reynolds numbers. *AIAA Journal* 20.4: 457-463.

Yarusevych S, Kawall JG and Sullivan PE(2008) Separated-shear-layer development on an airfoil at low Reynolds numbers. *AIAA journal* 46.12: 3060-3069.

Yarusevych S, Sullivan PE and Kawall JG (2009) On vortex shedding from an airfoil in low-Reynolds-number flows. *Journal of Fluid Mechanics* 632: 245-271.

Burgmann S, Brücker C and Schröder W (2006) W Scanning PIV measurements of a laminar separation bubble. *Experiments in Fluids* 41.2: 319-326.

Burgmann S and Schröder W (2008) Investigation of the vortex induced unsteadiness of a separation bubble via time-resolved and scanning PIV measurements. *Experiments in fluids* 45.4: 675-691.

Bai Peng, et al (2006) Numerical simulation of laminar separation bubble over 2D airfoil at low Reynolds number. *Acta Aerodyn Sin* 24.4: 416-24.

Fitzgerald EJ and Mueller TJ (1990). Measurements in a separation bubble on an airfoil using laser velocimetry. *AIAA journal* 28.4: 584-592.

Mohamed G (2001) Micro-air-vehicles: Can they be controlled better? *Journal of aircraft* 38.3: 419-429.

Mueller TJ (1985) The influence of laminar separation and transition on low Reynolds number airfoil hysteresis. *Journal of Aircraft* 22.9: 763-770.

Hu H, Yang ZF and Igarashi H (2007) Aerodynamic hysteresis of a low-Reynolds-number airfoil. *Journal of Aircraft* 44.6: 2083-2086.

Bai Peng et al (2015) Study about the non-linear and unsteady laminar separation phenomena around the airfoil at low reynolds number with low incidence. *Scientia Sinica Physica, Mechanica & Astronomica* 45.2: 4703.

Smith BL and Glezer A (1997) Vectoring and small-scale motions effected in free shear flows using synthetic jet actuators." *AIAA paper* 213: 1997.

Michael A, Smith BL and Glezer A (1998). Aerodynamic flow control using synthetic jet technology. *AIAA paper* 208: 1998.

Dovgal AV, Kozlov VV and Michalke (1994) A Laminar boundary layer separation: instability and associated phenomena. *Progress in Aerospace Sciences* 30.1: 61-94.